Forest Soil Amendment with *Morchella sextelata* Spent Substrate: Spatiotemporal Effects on Soil Properties and Microbial Communities in a Moso Bamboo Plantation

Baoxi Wang , Jinzong Xie * , Jian Zhang , Xin Wang

Posted Date: 28 February 2026

doi: 10.20944/preprints202602.2049.v1

Keywords: *Morchella sextelata* spent substrate; spent mushroom substrate (SMS); moso bamboo plantation soil; soil amendment; microbial community structure; enzyme-mediated nutrient cycling; high-throughput sequencing; soil depth effects

 doi:10.20944/preprints202602.2049.v1

Article

Forest Soil Amendment with *Morchella sextelata* Spent Substrate: Spatiotemporal Effects on Soil Properties and Microbial Communities in a Moso Bamboo Plantation

Baoxi Wang [1], Jinzong Xie [1,*], Jian Zhang [2] and Xin Wang [1]

[1] Research Institute of Subtropical Forestry, Chinese Academy of Forestry, Hangzhou 311400, China
[2] Forestry Bureau of Anji County, Huzhou 313300, China
* Correspondence: 13868141030@139.com; Tel.: +86-138-6814-1030 (J.X.)

Abstract

This study investigated the effects of different application rates of spent mushroom substrate (SMS) from *Morchella sextelata* on soil properties and microbial communities in a moso bamboo (*Phyllostachys edulis*) plantation. Three SMS rates (2.4, 4.7, and 9.4 kg·m^{-2}) were applied, and soil samples were collected at 6 and 12 months from two depths (0–20 cm and 20–40 cm). One year after application, topsoil total phosphorus (TP) increased 12–20 fold, while available phosphorus (AP) and potassium (AK) were significantly elevated. Soil pH initially decreased but partially recovered, whereas electrical conductivity (EC) continued to rise, indicating salt accumulation. Urease (UA) and sucrase (SA) activities increased 10–17 fold and 3–5 fold, respectively, while catalase (CAT) and acid phosphatase (ACP) were temporarily suppressed. SMS application significantly altered microbial community composition, with Acidobacteriota and Basidiomycota becoming more abundant. Correlation analysis identified pH, organic matter, AP, and UA as key factors linked to microbial changes. The medium application rate (4.7 kg·m^{-2}) provided the best balance between soil improvement and environmental risk. These findings demonstrate that *M. sextelata* SMS can effectively enhance soil fertility while modulating microbial communities, but salt accumulation and short-term acidification warrant attention.

Keywords: *Morchella sextelata* spent substrate; spent mushroom substrate (SMS); moso bamboo plantation soil; soil amendment; microbial community structure; enzyme-mediated nutrient cycling; high-throughput sequencing; soil depth effects

1. Introduction

Global production of edible mushrooms has exceeded 40 million tons annually, generating approximately 30 million tons of spent mushroom substrate (SMS) (estimated based on FAO 2025 data [1]; see also [2]). China accounts for over 70% of this production, making SMS disposal a critical environmental issue [1]. SMS typically contains high levels of organic matter, nitrogen, phosphorus, potassium, and bioactive compounds such as phenolics, terpenoids, and alkaloids [2,3]; thus, inappropriate disposal may impose environmental burdens, whereas its application as an organic soil amendment has been shown to improve soil structure, increase nutrient availability, and stimulate microbial and enzymatic activities [2,3]. Previous studies report that incorporating fungal residues into soils can reduce bulk density and increase water-holding capacity while significantly elevating soil organic matter, available phosphorus, and alkali-hydrolysable nitrogen; concomitantly, it enhances the activities of key enzymes such as urease, sucrase, and alkaline phosphatase, thereby facilitating soil ecological function recovery [4,5]. Moreover, SMS used as surface mulch can help stabilize soil pH and increase available potassium and phosphorus, demonstrating its potential for improving soils in agroforestry systems [6].

Morels (*Morchella* spp.) are highly valued edible fungi with rapidly expanding cultivation; consequently, the large amounts of nutrient-bag residues produced after harvest require sustainable

 doi:10.20944/preprints202602.2049.v1

utilization [7]. Morel fruiting bodies are rich in bioactive components, including polysaccharides, proteins, and polyphenols, and exhibit antioxidant, anti-inflammatory, and immunomodulatory properties [8,9]. The corresponding residues may retain fungus-derived bioactive substances, potentially conferring distinctive capacities for soil improvement and micro-ecological regulation [10,11]. Although some studies suggest that high-value compounds in SMS could be extracted for food or pharmaceutical applications [12,13], such extraction processes are currently not economically viable at the industrial scale required for the vast quantities of SMS generated annually. Therefore, direct soil application remains the most practical and environmentally beneficial route for bulk SMS utilization. Meanwhile, small-scale extraction for specialized high-value products and direct soil application can be pursued in parallel as complementary strategies, with the latter addressing the immediate need for large-scale waste management.

Moso bamboo (*Phyllostachys edulis*) is a key species in subtropical China, covering over 4.5 million hectares and providing both economic benefits (shoots, timber) and ecological services (carbon sequestration, water conservation) [14,15]. However, intensive management often leads to soil degradation, acidification, and nutrient imbalance, necessitating sustainable soil improvement practices [16]. Furthermore, *Morchella sextelata* SMS exhibits distinct compositional characteristics compared to other mushroom substrates. Our analysis (Table S4) shows that M. sextelata SMS contains 1443 ± 145 $mg \cdot kg^{-1}$ of total phosphorus, which is substantially higher than values reported for common wood-rotting mushroom species such as *Lentinula edodes* (800-1200 $mg \cdot kg^{-1}$) and *Pleurotus ostreatus* (700-1100 $mg \cdot kg^{-1}$) [4, Zhang et al. 2018]. This elevated phosphorus content may be attributed to the specific formulation of exogenous nutrient bags used in morel cultivation [2]. Additionally, as M. sextelata belongs to Ascomycota while most cultivated mushrooms are Basidiomycota, the composition of residual mycelia and associated secondary metabolites in the SMS may differ [8]. Although bioactive compounds have been identified in morel fruiting bodies and mycelia [10,11], their presence and potential ecological functions in the spent substrate have not been systematically investigated.

However, most existing studies focus on SMS applications in cropland systems or short-term effects [3,5]. Comprehensive evaluations of its performance and ecological consequences in forest ecosystems over a full annual cycle—particularly in economically and ecologically important moso bamboo plantations—remain limited [17]. Forest soil microbial communities are central to biogeochemical cycling and energy flow, and their composition, diversity, and functional activity are critical for maintaining soil health and supporting tree growth [18,19]. Inputs of exogenous organic materials can directly alter carbon and nitrogen substrate availability and indirectly impose selective pressures on soil microbial communities by modifying micro-environmental conditions such as pH and salinity [20]. It is important to note that SMS application may also entail potential risks; for example, some mushroom residues promote the accumulation of heavy metals such as chromium and cadmium in soils [21]. Moreover, introducing exogenous microorganisms may exert unintended impacts on indigenous microbial assemblages [22], a consideration particularly relevant in structurally complex forest ecosystems.

Research on fungus–forest interactions provides important insights into the potential ecological consequences of returning fungal residues to forest soils. Symbioses between ectomycorrhizal fungi and trees enhance nutrient acquisition, improve water relations, and increase host stress tolerance [23,24]. Studies on understory morel cultivation indicate that morels can modulate soil microbial communities and nutrient dynamics—for instance, reducing nitrate nitrogen while increasing the availability of certain mineral elements [7]. Some studies show that morel inoculation can promote maize growth and partially replace chemical fertilizers [25], suggesting that bioactive components or residual microorganisms in morel residues may influence woody plant performance through analogous mechanisms. Taken together, these findings imply that returning morel residues to forests is not only a waste-management approach but could also serve as a proactive strategy for soil ecological management.

 doi:10.20944/preprints202602.2049.v1

To address these knowledge gaps, we conducted a field experiment with graded SMS application rates, collecting soil samples from both topsoil (0–20 cm) and subsoil (20–40 cm) at 6 and 12 months post-application. By employing soil chemical assays, enzyme activity measurements, and high-throughput sequencing, we aimed to: (1) characterize the temporal dynamics and depth-specific differences in integrated fertility indicators and key soil enzyme activities following morel residue application; (2) quantify the effects of residue inputs on the structure, composition, and diversity of bacterial and fungal communities across soil layers and compare their response patterns; and (3) identify key environmental drivers of microbial successional trajectories, thereby providing a comprehensive evaluation of both soil-improvement benefits and potential ecological risks of forest application. The findings of this study provide a scientific basis for the safe, efficient, and resource-oriented utilization of morel residues in forestry production and contribute to forest soil health management.

2. Materials and Methods

2.1. Experimental Site and Materials

The experiment was conducted at the Hushan Forest Station of the Research Institute of Subtropical Forestry, Chinese Academy of Forestry, in Fuyang District, Hangzhou, Zhejiang Province (30°06′N, 119°56′E). A detailed map of the experimental site is provided in Figure S1 (Supplementary Materials). The region experiences a subtropical monsoon climate, with an average annual temperature of 16.1°C and average annual precipitation of 1442 mm. The experimental plantation consists of intensively managed pure moso bamboo (*Phyllostachys edulis*) stands, with understory vegetation coverage below 5%. The soil type is red soil developed from sandstone and shale parent material.

The spent substrate used in this study comprised residual nutrient bags from *Morchella sextelata* harvesting. The basic composition of the nutrient bag (dry weight ratio) included 60% barley grains, 40% bamboo shavings, 0.5% lime, 0.5% gypsum, and 0.5% monopotassium phosphate. Three random SMS samples were selected for basic nutrient analysis. Total nitrogen (TN) was determined by the Kjeldahl method, organic matter (SOM) by loss-on-ignition at 550°C, and total phosphorus (TP) by molybdenum-blue colorimetry after H_2SO_4-H_2O_2 digestion [26]. Results were: TN 0.87 ± 0.21%, SOM 34.90 ± 13.32%, and TP 1442.92 ± 144.95 mg·kg^{-1}. Detailed analytical results are provided in Table S4.

2.2. Experimental Design

The experiment followed a randomized complete block design with three blocks based on slope and initial soil nutrient heterogeneity. We established three SMS application rates: T1 (low, 2.4 kg·m^{-2}), T2 (medium, 4.7 kg·m^{-2}), and T3 (high, 9.4 kg·m^{-2}). The doses were selected based on local farmer practice for semi-wild morel cultivation in bamboo forests, where a typical application rate is approximately 4–5 kg·m^{-2} (referred to as medium, T2). To explore the dose–response relationship, we set a low dose (T1, approximately half of T2) and a high dose (T3, approximately double T2), resulting in a doubling pattern (T2 ≈ 2×T1, T3 ≈ 2×T2). This design is commonly used in agronomic trials to detect nonlinear responses and to identify optimal application rates [8,25]. Each treatment was replicated three times, resulting in nine experimental plots, each measuring 16 m^2 (4 m × 4 m). The SMS was evenly spread on the soil surface in October 2023, followed by manual shallow tilling to a depth of 5–10 cm (controlled by using a fixed-depth cultivator set to 7.5 cm, operated by the same technician to minimize variation). Although SMS was incorporated only into the top 5–10 cm, soluble nutrients and microbial metabolites released during decomposition can leach downward, affecting subsoil (20–40 cm) properties over time. This mechanism has been documented in organic amendment studies [27].

2.3. Sample Collection and Processing

Soil samples were collected before SMS application (October 2023, Initial I), and at 6 months (April 2024, M) and 12 months (October 2024, F) after application. Within each plot, we used a five-point sampling method to collect soil from the 0–20 cm (topsoil, S) and 20–40 cm (subsoil, D)

 doi:10.20944/preprints202602.2049.v1

layers using a stainless steel soil auger (5 cm diameter). Five subsamples from each layer within the same plot were combined into a composite sample in sterile polyethylene bags. This compositing was performed to obtain a representative sample for each plot and to reduce random spatial variability, a common practice in soil ecological studies [28]. Samples were immediately placed in a cooling box and transported to the laboratory within 4 hours.

Each composite sample was processed as follows: (1) A portion of fresh soil was passed through a 2-mm sterile nylon sieve, divided into aliquots, and stored at –80°C for subsequent total soil DNA extraction. (2) Another portion was sieved through a 2-mm mesh and stored at 4°C for enzyme activity measurements completed within one week. (3) The remaining samples were air-dried in a shaded, well-ventilated area. After removing stones and plant debris, we ground and passed them through 2-mm and 0.149-mm nylon sieves, then sealed them for soil physicochemical property analysis.

2.4. Measurement Indicators and Methods

2.4.1. Soil Physicochemical Property Measurements

Soil pH was measured using a potentiometric method (soil:water ratio 1:2.5). Electrical conductivity (EC) was measured using a conductivity meter (soil:water ratio 1:5). Soil organic matter (SOM) was determined by the potassium dichromate oxidation method, and total nitrogen (TN) was measured using the Kjeldahl method. Total phosphorus (TP) was quantified by sodium hydroxide fusion-molybdenum-antimony colorimetry, and total potassium (TK) was measured using sodium hydroxide fusion-flame photometry. Alkali-hydrolysable nitrogen (AN) was determined by the alkali diffusion method. Available phosphorus (AP) was measured using sodium bicarbonate extraction-molybdenum-antimony colorimetry, and available potassium (AK) was determined by ammonium acetate extraction-flame photometry. All analyses were performed in triplicate with quality control using certified reference materials.

2.4.2. Soil Enzyme Activity Measurements

Urease (UA) activity was determined by phenol-sodium hypochlorite colorimetry: 5 g soil was incubated with 10 mL 10% urea solution at 37°C for 24 h, and released NH_3-N was measured at 578 nm [29]. Sucrase (SA) activity was assayed by 3,5-dinitrosalicylic acid method: 5 g soil incubated with 15 mL 8% sucrose at 37°C for 24 h, and glucose released was quantified at 508 nm [29]. Acid phosphatase (ACP) was measured using disodium phenyl phosphate: 5 g soil incubated with 20 mL 0.5% substrate at 37°C for 2 h, and phenol released was determined at 510 nm [30]. Catalase (CAT) activity was measured by $KMnO_4$ titration after incubating soil with H_2O_2 [31]. Acid protease (APR) was assayed using casein as substrate, with tyrosine release measured at 680 nm [32]. For all assays, controls without substrate were included to correct for non-enzymatic reactions.

2.4.3. Microbial Community Analysis

Total soil DNA was extracted from 0.5 g fresh soil using the FastDNA® Spin Kit for Soil (MP Biomedicals, USA). The bacterial 16S rRNA gene V3-V4 region was amplified by PCR using universal primers 338F (5′-ACTCCTACGGGAGGCAGCAG-3′) and 806R (5′-GGACTACHVGGGTWTCTAAT-3′). The fungal ITS1 region was amplified using primers ITS1F (5′-CTTGGTCATTTAGAGGAAGTAA-3′) and ITS2R (5′-GCTGCGTTCTTCATCGATGC-3′). The amplified products were purified, quantified, and normalized before sequencing on the Illumina NovaSeq 6000 platform with 2×250 bp paired-end sequencing (contracted through Guangzhou Gidiou Biotechnology Co., Ltd.). Raw sequencing data were processed on the Omicssmart platform for quality control, including primer removal and filtering of low-quality sequences. The DADA2 algorithm was employed for denoising and generating Amplicon Sequence Variants (ASVs). Bacterial and fungal ASVs were classified taxonomically based on the SILVA database (release 138.1) and the UNITE database (version 8.3), respectively. To minimize sequencing depth discrepancies, all samples were rarefied to the lowest sequence count.

 doi:10.20944/preprints202602.2049.v1

2.5. Data Analysis

Soil physicochemical properties and enzyme activity data were expressed as the mean ± standard deviation from three biological replicates. To account for repeated measures and the lack of a true control, data were analyzed using linear mixed-effects models (LMM) with the 'nlme' package in R (version 4.3.1). Treatment, time (as categorical), and soil layer were included as fixed factors, while plot was included as a random intercept to account for temporal autocorrelation. Initial values (I period) were used as a covariate to adjust for baseline differences. Significant main effects and interactions were further examined using Tukey's HSD post-hoc tests ($\alpha = 0.05$). Different letters indicate significant differences between treatment–time–layer combinations ($p < 0.05$). Full results of the linear mixed models, including all two-way and three-way interactions, are provided in Table S2 (Supplementary Materials). Interaction plots for key variables are presented in Figures S2–S4.

To identify key environmental factors driving microbial community changes, Spearman correlation coefficients were calculated between the relative abundances of major bacterial and fungal phyla (relative abundance >1%) and selected core environmental factors (pH, organic matter [OM], alkali-hydrolysable nitrogen [AN], available phosphorus [AP], and urease activity [URE]). Spearman's rank correlation was chosen because preliminary analysis indicated that several environmental variables and microbial phyla abundances were not normally distributed (Shapiro-Wilk test, $p < 0.05$). Spearman's correlation is a non-parametric measure that does not assume normality and is robust to outliers, making it more appropriate for this dataset. Additionally, it captures monotonic relationships, which are common in ecological data where responses may be nonlinear but consistently directional [33]. Correlation significance was assessed using the 'rcorr' function in R (Hmisc package) with Bonferroni correction for multiple comparisons.

Principal coordinate analysis (PCoA) based on the Bray-Curtis dissimilarity matrix was conducted using the 'vegan' package in R, and differences in microbial community structure across groups were tested by permutational multivariate analysis of variance (PERMANOVA, Adonis function, 999 permutations). Linear discriminant analysis effect size (LEfSe) with a threshold of LDA score ≥ 3.0 was used to identify statistically significant biomarker taxa between groups. All statistical analyses were performed in R (version 4.3.1), with plots generated primarily using the 'ggplot2' package.

3. Results

3.1. Spatiotemporal Effects of Spent Substrate Application on Soil Physicochemical Properties

Spent substrate application significantly altered the chemical properties of both soil layers, with effects showing distinct spatiotemporal heterogeneity. One year after application (F), TP content in the topsoil peaked, with T1, T2, and T3 treatments reaching 531.2 ± 11.4, 520.6 ± 8.0, and 749.6 ± 54.3 $mg{\cdot}kg^{-1}$, respectively, representing 13.9, 12.1, and 20.4 times initial values (I). TP content in the subsoil also increased significantly, with F-period values for T1, T2, and T3 treatments of 383.2 ± 3.5, 400.6 ± 15.9, and 401.9 ± 9.9 $mg{\cdot}kg^{-1}$, respectively—an increase of approximately 12–13 times, though still significantly lower than corresponding topsoil values.

The trends in available phosphorus (AP) and available potassium (AK) resembled those of TP, with both increasing significantly after application, and the increase generally greater in topsoil than subsoil. Six months after application (M), AP in the topsoil decreased, then rebounded significantly by the F-period. AK in the topsoil increased sharply at M-period, reaching 2.8–3.6 times initial values for T1, T2, and T3 treatments. Although it decreased slightly in the F-period, it remained significantly higher than initial levels. The increases in AP and AK in the subsoil were more gradual.

Soil pH declined significantly six months after application, with topsoil pH dropping from 7.45–8.22 to 5.46–5.50—a reduction of approximately 2 units, indicating marked acidification. Subsoil pH also decreased from 5.56–6.05 to 5.33–6.00. By the F-period (one year after application), topsoil pH partially recovered to 6.56–6.58, and subsoil pH to 6.59–6.64, though both remained below initial levels. Electrical conductivity (EC) showed a continuous increasing trend, with topsoil EC values rising sharply in the F-period, reaching 324.67 ± 19.06, 331.33 ± 26.08, and 350.67 ± 12.50 $\mu S{\cdot}cm^{-1}$

 doi:10.20944/preprints202602.2049.v1

for T1, T2, and T3 treatments, approximately 15–20 times initial values. Although EC in the subsoil increased, it remained significantly lower than in the topsoil, indicating that soluble salts from SMS decomposition primarily accumulated in the surface layer.

Linear mixed model analysis revealed that time exerted a highly significant effect ($p < 0.001$) on all physicochemical indicators. The soil layer effect was highly significant ($p < 0.001$) for all indicators except total potassium (TK). The treatment effect was primarily evident in indicators such as TP, AP, AK, and EC. Significant interactions (e.g., Time × Layer) indicated that the impact patterns of different application rates on soil properties varied over time, and temporal effects differed between topsoil and subsoil.

Table 1. Temporal Changes in Key Physicochemical Properties of Topsoil and Subsoil Under Spent Substrate Application.

Trt	Layer	Period	OM (%)	TN (mg/kg)	TP (mg/kg)	AN (mg/kg)	AP (mg/kg)	AK (mg/kg)	pH	EC (μS/cm)
T1	S	I	1.74±0.08^{a}	478.9±85.4^{a}	38.2±8.7^{a}	51.3±1.4^{a}	51.8±4.6^{a}	117.2±11.7^{a}	8.22±0.11^{a}	16.55±2.33^{a}
T1	S	M	0.65±0.03^{g}	666.8±11.1^{f}	53.6±6.8^{g}	50.3±4.6^{a}	15.8±0.5^{d}	328.3±7.8^{f}	5.50±0.17^{g}	43.43±8.40^{e}
T1	S	F	0.39±0.06^{m}	317.8±16.6^{k}	531.2±11.4^{k}	29.3±0.6^{g}	46.2±1.9^{g}	189.1±4.6^{h}	6.56±0.02^{j}	324.67±19.06^{j}
T1	D	I	0.52±0.08^{b}	276.6±22.8^{b}	31.4±3.1^{b}	15.1±4.2^{b}	10.4±1.1^{b}	61.5±4.8^{b}	6.05±0.19^{b}	19.75±2.29^{b}
T1	D	M	0.58±0.02^{h}	544.9±16.9^{g}	36.8±1.6^{e}	21.5±1.3^{f}	11.8±0.7^{b}	88.9±3.4^{g}	6.00±0.08^{b}	52.10±13.79^{f}
T1	D	F	0.26±0.05^{n}	239.0±16.7^{l}	383.2±3.5^{l}	24.3±2.2^{i}	50.1±3.1^{h}	106.3±7.8^{j}	6.64±0.04^{k}	438.33±126.87^{k}
T2	S	I	2.00±0.10^{c}	571.1±86.7^{c}	43.1±4.3^{c}	63.1±3.9^{c}	50.7±7.0^{a}	108.7±11.5^{c}	7.67±0.09^{c}	19.70±2.50^{b}
T2	S	M	0.86±0.03^{i}	1165.2±50.1^{h}	49.9±1.8^{h}	51.2±1.8^{a}	14.2±0.8^{e}	192.5±9.6^{h}	5.46±0.14^{g}	41.70±8.72^{e}
T2	S	F	0.49±0.07^{o}	404.8±22.9^{m}	520.6±8.0^{m}	42.6±2.1^{j}	48.4±1.3^{i}	219.5±4.9^{k}	6.58±0.03^{j}	331.33±26.08^{j}
T2	D	I	0.99±0.22^{d}	437.8±59.4^{d}	35.1±1.2^{d}	26.8±6.0^{d}	9.9±0.9^{b}	67.1±2.3^{d}	5.86±0.06^{d}	16.87±2.53^{c}
T2	D	M	0.68±0.04^{j}	869.4±24.0^{i}	40.4±1.7^{i}	29.6±0.9^{g}	10.8±0.4^{b}	98.8±3.5^{i}	5.65±0.15^{h}	33.03±4.27^{g}
T2	D	F	0.35±0.02^{p}	336.7±10.5^{n}	400.6±15.9^{n}	31.8±2.2^{k}	48.5±2.1^{i}	114.2±3.7^{l}	6.59±0.04^{j}	332.00±26.54^{j}
T3	S	I	2.18±1.10^{e}	495.8±54.9^{e}	36.8±1.6^{e}	50.9±12.8^{a}	52.4±3.8^{c}	91.0±27.2^{e}	7.45±0.18^{e}	18.71±5.17^{b}
T3	S	M	0.79±0.03^{k}	891.4±27.2^{j}	62.0±2.9^{j}	37.3±0.5^{h}	15.7±0.7^{d}	195.5±5.4^{h}	5.49±0.09^{g}	36.73±2.48^{h}
T3	S	F	0.40±0.03^{q}	390.9±14.3^{o}	749.6±54.3^{o}	41.9±1.9^{j}	46.9±2.2^{g}	180.4±8.6^{m}	6.58±0.01^{j}	350.67±12.50^{l}
T3	D	I	0.66±0.13^{f}	281.9±98.8^{b}	29.8±0.6^{f}	19.9±1.0^{e}	11.2±2.0^{b}	67.2±1.5^{d}	5.56±0.11^{f}	23.96±5.40^{d}
T3	D	M	0.61±0.02^{l}	665.5±20.8^{f}	49.5±0.7^{h}	23.8±0.4^{i}	12.8±0.4^{f}	108.5±2.3^{j}	5.33±0.07^{i}	28.73±0.64^{i}
T3	D	F	0.24±0.01^{r}	278.9±12.0^{l}	401.9±9.9^{n}	28.0±1.6^{l}	45.2±1.2^{j}	114.7±7.1^{l}	6.62±0.02^{k}	270.33±26.21^{m}

Data are presented as means ± standard deviation (n = 3). Different superscript letters within the same column indicate significant differences between treatments ($p < 0.05$). OM = organic matter; TN = total nitrogen; TP = total phosphorus; AN = alkali-hydrolysable nitrogen; AP = available phosphorus; AK = available potassium; EC = electrical conductivity. Linear mixed models showed significant or highly significant main effects and interactions of treatment, time, and soil layer on indicators such as total phosphorus, available phosphorus, available potassium, pH, and electrical conductivity ($p < 0.05$ or $p < 0.001$; see Table S2 for full results).

3.2. Spatiotemporal Effects of Spent Substrate Application on Soil Enzyme Activities

SMS application significantly affected the activities of key enzymes involved in carbon, nitrogen, and phosphorus cycling as well as redox reactions in both soil layers, with notable spatiotemporal and depth-dependent response patterns.

Urease (UA) and sucrase (SA) activities increased significantly in both soil layers, with much greater enhancement in topsoil than subsoil. Peak activities occurred one year after application (F), indicating a lagged stimulation effect. Catalase (CAT) activity showed a different trend: six months after application (M), CAT activity in the topsoil of all treatments decreased significantly compared to initial values; by the F-period, though partially recovered, it remained significantly lower than initial levels (see Table 2). Subsoil CAT activity changes were relatively gradual. Acid phosphatase (ACP) activity in topsoil was generally lower than initial values at M-period but partially recovered by F-period. This response pattern resembles that of CAT, suggesting both enzymes may have responded jointly to intense microbial metabolic disturbances during early SMS decomposition. Acid protease (APR) activity showed variable responses at M-period, but by F-period, APR activity in topsoil across all treatments was significantly lower than initial levels.

Linear mixed model analysis showed that time and soil layer both exerted highly significant effects ($p < 0.001$) on all measured enzyme activities. Treatment significantly affected urease (UA), sucrase (SA), and acid protease (APR) activities ($p < 0.05$). A significant Time × Layer interaction indicated temporal changes in enzyme activity differed between soil layers, with topsoil enzyme activities responding more sensitively and intensely to SMS application.

 doi:10.20944/preprints202602.2049.v1

Table 2. Temporal Changes in Key Soil Enzyme Activities in Topsoil and Subsoil Under Spent Substrate Application.

Trt	Layer	Period	UA (U/g)	SA (U/g)	ACP (nmol/d/g)	CAT (μmol/d/g)	APR (U/g)
T1	S	I	13.9 ± 1.6^{a}	127.8 ± 21.4^{a}	503.8 ± 33.0^{a}	45.3 ± 6.8^{a}	188.5 ± 36.7^{a}
T1	D	I	6.9 ± 2.9^{b}	48.2 ± 18.0^{b}	421.9 ± 20.0^{b}	50.4 ± 15.2^{b}	211.5 ± 35.1^{b}
T2	S	I	23.9 ± 9.8^{c}	155.2 ± 26.9^{c}	482.4 ± 40.5^{c}	49.2 ± 8.4^{c}	158.7 ± 28.7^{c}
T2	D	I	15.2 ± 7.4^{d}	48.4 ± 8.1^{b}	406.6 ± 25.4^{d}	72.7 ± 11.9^{d}	178.4 ± 25.4^{d}
T3	S	I	19.4 ± 9.2^{e}	140.0 ± 31.8^{d}	559.0 ± 104.1^{e}	39.3 ± 3.7^{e}	171.3 ± 87.3^{e}
T3	D	I	8.2 ± 4.7^{f}	46.4 ± 23.8^{b}	502.7 ± 101.3^{f}	59.3 ± 23.8^{f}	162.8 ± 39.0^{f}
T1	S	M	39.3 ± 1.0^{g}	21.5 ± 1.6^{e}	260.6 ± 12.4^{g}	26.0 ± 1.3^{g}	198.0 ± 10.2^{a}
T1	D	M	35.5 ± 1.3^{h}	14.5 ± 1.2^{f}	241.5 ± 3.5^{h}	51.2 ± 1.8^{b}	175.0 ± 5.6^{d}
T2	S	M	42.1 ± 0.6^{i}	23.9 ± 0.3^{g}	253.6 ± 5.1^{i}	43.3 ± 4.6^{a}	157.9 ± 10.6^{c}
T2	D	M	39.3 ± 0.7^{g}	16.8 ± 0.4^{h}	236.2 ± 5.8^{j}	58.2 ± 1.3^{f}	139.5 ± 3.5^{g}
T3	S	M	43.6 ± 0.8^{j}	17.6 ± 0.5^{i}	264.6 ± 9.9^{g}	42.2 ± 2.4^{a}	159.3 ± 4.8^{c}
T3	D	M	41.8 ± 0.8^{k}	12.7 ± 0.4^{j}	250.5 ± 2.1^{k}	60.5 ± 1.9^{h}	130.7 ± 1.9^{h}
T1	S	F	212.9 ± 6.4^{l}	546.7 ± 3.1^{k}	354.2 ± 6.2^{l}	26.99 ± 8.66^{g}	89.8 ± 6.0^{i}
T1	D	F	63.2 ± 4.2^{m}	317.6 ± 6.2^{l}	354.2 ± 6.2^{l}	37.08 ± 9.00^{i}	90.9 ± 5.9^{i}
T2	S	F	245.2 ± 18.9^{n}	780.1 ± 21.6^{m}	361.7 ± 19.0^{m}	22.27 ± 4.55^{j}	86.8 ± 8.3^{j}
T2	D	F	77.3 ± 6.4^{o}	478.7 ± 29.3^{n}	361.7 ± 19.0^{m}	42.12 ± 5.13^{k}	86.8 ± 8.3^{j}
T3	S	F	221.1 ± 11.4^{p}	641.8 ± 38.8^{o}	348.0 ± 20.2^{n}	23.24 ± 6.04^{l}	79.9 ± 6.9^{k}
T3	D	F	80.4 ± 7.1^{q}	488.5 ± 38.1^{p}	348.0 ± 20.2^{n}	45.58 ± 5.48^{m}	79.9 ± 6.9^{k}

Data are presented as means ± standard deviation (n = 3). Different superscript letters within the same column indicate significant differences between treatments ($p < 0.05$). UA = urease activity; SA = sucrase activity; ACP = acid phosphatase; CAT = catalase activity; APR = acid protease activity. Linear mixed models showed significant effects of time and soil layer on urease, sucrase, and acid phosphatase activities ($p < 0.001$), and treatment significantly affected urease and sucrase activities ($p < 0.05$).

3.3. Effects of Spent Substrate Application on Soil Microbial Community Composition

SMS input significantly altered microbial community composition in both topsoil and subsoil. The bacterial community was predominantly composed of Acidobacteriota, Chloroflexota, Pseudomonadota, and Actinomycetota (Figure 1A). After application, the relative abundance of Acidobacteriota generally increased in later samples (M, F), particularly in topsoil. For instance, in T2-treated topsoil, Acidobacteriota abundance increased from 24% initially to 30% at F-period. Pseudomonadota relative abundance also increased in topsoil, especially in F-period samples from T1 and T2 treatments. Actinomycetota and Planctomycetota relative abundances decreased after substrate application.

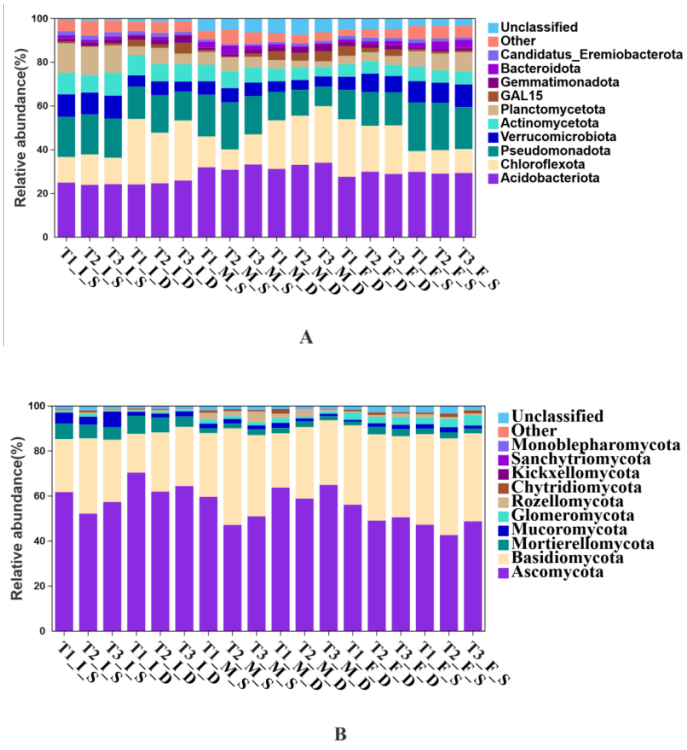

Figure 1. Effects of *Morchella sextelata* spent substrate application on soil microbial community composition at the phylum level. (A) Bacterial community composition (stacked bar plot); (B) Fungal community composition (stacked bar plot). Samples are arranged by treatment (T1, T2, T3), period (I: Initial, M: 6 months post-application, F: 12 months post-application), and soil layer (S: Topsoil, D: Subsoil). Axis labels have been enlarged and rotated 45° for improved readability.

 doi:10.20944/preprints202602.2049.v1

The fungal community was dominated by Ascomycota and Basidiomycota (Figure 1B). One year after application (F), Basidiomycota relative abundance increased significantly in both soil layers compared to initial period (I), while Ascomycota abundance decreased correspondingly. For example, in T2-treated topsoil, Basidiomycota increased dramatically from 33% initially to 43% at F-period, while Ascomycota decreased from 52% to 43%. Mortierellomycota and Mucoromycota relative abundances generally decreased after substrate application. Subsoil microbial community composition trends resembled topsoil but with generally smaller magnitude changes, reflecting persistent influence of soil vertical gradients on microbial distribution.

3.4. Effects of Spent Substrate Application on Soil Microbial Community Structure

Principal coordinate analysis (PCoA) based on Bray-Curtis distances further revealed overall changes in microbial community structure induced by SMS application (Figure 2). For bacterial communities (Figure 2A), the first (PCo1) and second (PCo2) principal coordinates explained 22.10% and 17.79% of total variation, respectively. PERMANOVA confirmed time (sampling period) was the primary factor driving bacterial community structure variation ($R^2 = 0.35$, $p = 0.001$), with soil layer also significant ($R^2 = 0.15$, $p = 0.001$). In the PCoA plot, initial (I), 6-month post-application (M), and 12-month post-application (F) samples formed distinct separation trajectories in ordination space. Within the same sampling period, topsoil (S) and subsoil (D) samples also showed partial separation, indicating persistent influence of vertical soil heterogeneity on community assembly.

For fungal communities (Figure 2B), PCo1 and PCo2 explained 13.09% and 9.23% of total variation, respectively. Similarly, PERMANOVA showed time was the strongest driver of fungal community structure ($R^2 = 0.28$, $p = 0.001$), with soil layer also significant ($R^2 = 0.12$, $p = 0.001$). Samples from different periods separated clearly, and topsoil and subsoil samples exhibited separation within respective period groups. Differences among treatments (T1, T2, T3) were less pronounced in ordination space compared to time and soil layer effects, indicating that the event of SMS addition itself and associated temporal environmental changes had stronger influence on overall community structure than application rate differences in this study.

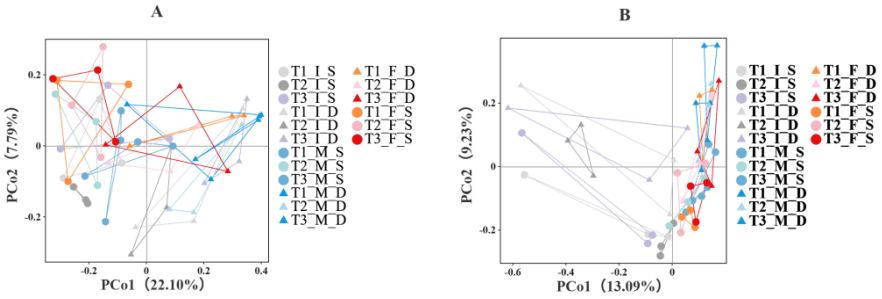

Figure 2. Principal coordinate analysis (PCoA) of soil microbial communities based on Bray-Curtis distances. (A) Bacterial community PCoA plot (PCo1: 22.10%, PCo2: 17.79%). PERMANOVA indicated time ($R^2 = 0.35$, $p = 0.001$) was the primary significant factor driving bacterial community structure variation. (B) Fungal community PCoA plot (PCo1: 13.09%, PCo2: 9.23%). PERMANOVA indicated time ($R^2 = 0.28$, $p = 0.001$) and soil layer ($R^2 = 0.12$, $p = 0.001$) significantly influenced fungal community structure. Points represent samples, with color indicating sampling period (I: gray, M: blue, F: red) and shape indicating soil layer (circle: topsoil S; triangle: subsoil D).

3.5. Correlation Analysis Between Soil Microbial Communities and Environmental Factors

To identify key environmental factors driving microbial community changes, we calculated Spearman correlation coefficients between major bacterial and fungal phyla and selected core environmental factors (pH, organic matter [OM], alkali-hydrolysable nitrogen [AN], available phosphorus [AP], and urease activity [URE]) (Figure 3).

Bacterial community correlation analysis (Figure 3A) revealed significant differentiation in how different bacterial phyla responded to environmental factors. Planctomycetota showed strong positive correlations with soil pH ($r = 0.697$), organic matter ($r = 0.698$), alkali-hydrolysable nitrogen ($r =$

 doi:10.20944/preprints202602.2049.v1

0.676), available phosphorus (r = 0.741), and urease activity (r = 0.036). Actinomycetota showed strong positive correlations with organic matter (r = 0.687) and available phosphorus (r = 0.561). Acidobacteriota showed a moderate negative correlation with pH (r = –0.451). Chloroflexota showed negative correlations with most nutrient indicators (AN, AP, AK) and urease activity.

Fungal community correlation analysis (Figure 3B) also revealed functional differentiation. Basidiomycota showed positive correlations with total phosphorus (r = 0.384), available potassium (r = 0.323), and urease activity (r = 0.458). Ascomycota showed negative correlation trends with most nutrient indicators. Mortierellomycota showed a positive correlation with pH (r = 0.338) but a negative correlation with total phosphorus (r = –0.538).

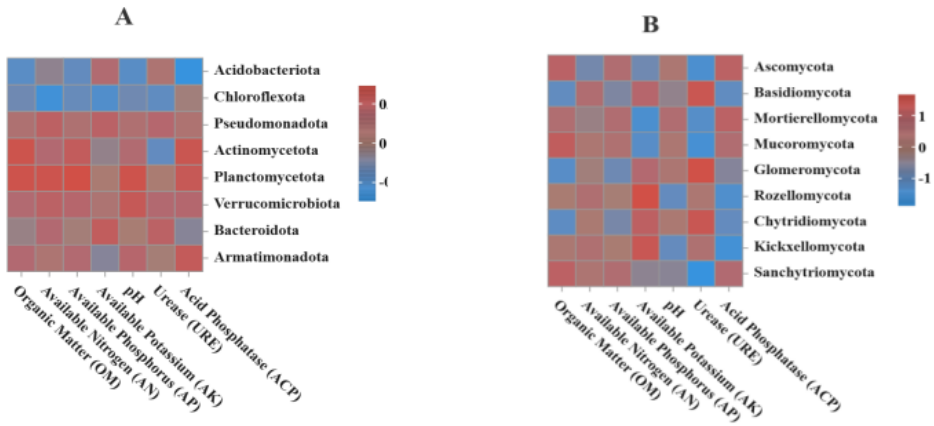

Figure 3. Spearman correlation heatmap of major soil microbial phyla (phylum level) and key environmental factors. (A) Correlations between major bacterial phyla and key environmental factors; (B) Correlations between major fungal phyla and key environmental factors. Color represents correlation coefficient strength (red: positive, blue: negative). Color intensity reflects correlation strength, with * indicating $p < 0.05$ and ** indicating $p < 0.01$. Only major phyla with relative abundance >1% are shown.

4. Discussion

Through this one-year field experiment, we systematically elucidated the multidimensional effects of amending soil with *Morchella sextelata* SMS on physicochemical properties, multifunctional enzyme activities, and microbial communities in bamboo forest topsoil and subsoil.

The addition of SMS directly and substantially altered soil chemistry, most notably inducing a sharp and significant increase in the total phosphorus (TP) pool in both soil layers. This pronounced effect closely related to the high phosphorus content (1442.92 $mg \cdot kg^{-1}$) of the SMS itself. This finding aligns with numerous studies concluding that mushroom residues effectively enhance soil available phosphorus [4,5]. The significant increase in phosphorus likely resulted from rapid mineralization of organic phosphorus combined with activation of soil's inherent insoluble phosphorus by decomposition products [23]. Notably, phosphorus accumulated more in topsoil than subsoil, indicating some downward migration. Nevertheless, a clear surface accumulation effect was observed, likely because the substrate was mainly surface-applied, and migration of its decomposition products and released phosphate ions was restricted by soil colloidal adsorption, plant absorption, and microbial fixation [24].

Following SMS application, soil pH initially decreased significantly, then partially recovered after one year; the initial acidification likely linked to organic acid production during substrate decomposition and enhanced nitrification. Concurrently, EC showed a continuous upward trend, reflecting soluble salt accumulation in the surface layer, attributable to inherent salt content (e.g., K^+) in the SMS and its mineralization and release processes. This observation highlights that potential soil salinity accumulation risk should be considered during long-term or high-dose SMS applications, especially in low-rainfall or poor-drainage areas. Similarly, previous studies note potential heavy metal accumulation risks from mushroom residue application [21]. Although this study did not monitor

 doi:10.20944/preprints202602.2049.v1

heavy metals, it remains crucial to screen SMS sources for heavy metals before large-scale application to ensure environmentally safe resource utilization [3].

4.1. Synergistic and Differential Responses of Soil Multifunctional Enzyme Activities

SMS application induced clear functional specificity, spatiotemporal heterogeneity, and a "surface effect" in soil enzyme activities. Urease (UA) and sucrase (SA) activities peaked in topsoil one year after application, attributable to continuous decomposition of carbon and nitrogen substrates from SMS and subsequent formation of a stable microenvironment conducive to synthesis of related hydrolytic enzymes [25,26]. In contrast, catalase (CAT) and acid phosphatase (ACP) activities were significantly reduced in topsoil six months after application. The reduction in CAT activity may be related to increased consumption of H_2O_2 by rapidly proliferating microorganisms during the early stages of decomposition, reflecting dynamic adjustments in soil oxidative metabolism [27]. The initial suppression of ACP activity may be associated with the elevated available phosphorus levels resulting from SMS decomposition, potentially reflecting a net decrease in phosphatase production or increased enzyme degradation under conditions of high phosphorus availability [28]. However, soil enzyme activity represents the cumulative outcome of synthesis, stabilization, and degradation processes; further studies at the gene expression level are needed to elucidate the underlying mechanisms. Acid protease (APR) activity generally decreased after one year, suggesting SMS input altered soil nitrogen cycling pathways. On one hand, SMS is rich in organic nitrogen, and its mineralization directly increased inorganic nitrogen supply, possibly reducing reliance on protein hydrolysis. On the other hand, microbial community succession (e.g., Basidiomycota enrichment) may have favored utilization of other nitrogen forms. This differential response suggests SMS input did not simply activate all soil biological activity but induced functional redistribution within the soil ecosystem: strongly promoting carbon and nitrogen hydrolysis while causing short-term inhibition or long-term downregulation of phosphorus hydrolysis and oxidative stress-related enzyme activities. This represents sophisticated functional reconfiguration in response to exogenous organic matter input.

4.2. Functional Directional Succession of Microbial Communities

Microbial community evolution provides the biological basis for aforementioned environmental and enzyme activity changes. PCoA analysis indicates time (successional process) as the primary driving factor [29]. Acidobacteriota enrichment in bacterial communities aligns with its characteristics as an oligotrophic K-strategist efficient at degrading complex lignocellulose in SMS [20]. The marked increase in Basidiomycota within fungal communities holds key ecological significance. This phylum contains many lignin-degrading fungi [30], and its growth directly responds to bamboo chip substrate in SMS, likely playing a leading role in decomposing recalcitrant carbon components in later stages. This change potentially links to acid phosphatase and catalase activity changes. Basidiomycota fungi often produce H_2O_2 during lignin breakdown and rely on peroxidase systems, possibly causing competition for CAT substrates or metabolic bypasses. Simultaneously, their ability to mineralize organic phosphorus may partially replace soil inherent ACP function. Subsoil microbial community changes were less pronounced, confirming the "surface effect" of enzyme activity changes and reflecting persistent influence of vertical soil heterogeneity [31,32].

4.3. Environmental Factor-Driven "Functional-Community" Association Network

Correlation analysis and key factor identification further elucidated underlying relationships. Soil pH, organic matter, available phosphorus, and urease activity were core environmental factors co-varying with key groups such as Planctomycetota, Actinomycetota, and Basidiomycota. Initial acidification favored acidophilic microorganisms (e.g., Acidobacteriota), while subsequent nutrient availability increases shaped functional communities in later stages. Notably, catalase activity negatively correlated with some fungal groups, possibly revealing inherent trade-offs between active lignin degradation processes and H_2O_2 metabolism. The proposed framework of "SMS input $\rightarrow$ environmental factor changes (pH, nutrients) $\rightarrow$ differential enzyme activity responses $\rightarrow$ shifts in

 doi:10.20944/preprints202602.2049.v1

microbial community composition" summarizes the correlational patterns observed in this study and provides a conceptual model for how SMS application may influence soil ecological functions. Further experimental studies are needed to validate the causal relationships implied in this framework.

4.4. Practical Implications and Prospects

From a practical perspective, although high-dose application (T3) demonstrated highest potential for increasing total phosphorus, medium-dose application (T2) achieved similar or even better effects in improving available nutrients, stimulating enzyme activity, and regulating microbial communities, while likely posing lower environmental risks (e.g., surface salt accumulation). Therefore, considering benefit–risk balance, we recommend medium-dose application (4.7 $kg \cdot m^{-2}$) as the optimized practice for *Morchella sextelata* SMS in moso bamboo forest soil improvement. Our findings also indicate that short-term soil acidification induced by SMS application warrants attention. Although pH partially recovered within one year, it remained below initial levels. In regions with inherently acidic soils or where rapid pH adjustment is desired, supplementary practices such as lime application may be considered to mitigate acidification effects. Significant improvement in subsoil nutrients indicates SMS effects can penetrate to certain depth, beneficial for enhancing deep soil fertility and promoting deep root growth in bamboo forests [7,33].

A limitation of this study is the one-year experimental period, which did not reveal long-term fate of SMS effects. Additionally, functional inferences based on correlation analysis are somewhat indicative. Future studies should extend monitoring periods to reveal long-term dynamics of SMS effects. Moreover, metagenomics, transcriptomics, and stable isotope probing should be employed to further validate specific functions of key microbial groups [34]. Comprehensive screening of heavy metals and persistent organic pollutants in SMS is also necessary to assess long-term environmental safety. Ultimately, integrating SMS into sustainable forest resource recycling systems requires comprehensive consideration of local environmental conditions, tree species characteristics, and management objectives. As emphasized by [35], balancing technical feasibility with economic-ecological benefits is key to achieving sustainable utilization.

5. Conclusions

This one-year field experiment systematically clarified the effects of *Morchella sextelata* spent substrate on bamboo forest soil ecosystems and elucidated underlying microbiological mechanisms. The main conclusions are:

(1) *Morchella sextelata* SMS amendment rapidly and significantly enhanced soil phosphorus and potassium nutrients, exhibiting pronounced surface accumulation while also impacting deeper soil layers. Soil pH initially decreased significantly then partially recovered, whereas continuous electrical conductivity increases indicate potential salt accumulation risk.

(2) SMS application demonstrated clear functional specificity in soil enzyme activity. Urease and sucrase activities were strongly stimulated, thereby enhancing carbon and nitrogen cycling. However, catalase and acid phosphatase activities showed short-term suppression, reflecting initial perturbations in soil oxidative metabolism and phosphorus transformation pathways. Long-term acid protease decline suggests alteration in organic nitrogen mineralization pathways.

(3) SMS application drove functional succession of microbial communities, with Acidobacteriota (bacteria) and Basidiomycota (fungi) at the core. The former utilizes complex carbon sources efficiently, while the latter dominates lignin degradation. Together, they facilitated spent substrate decomposition and transformation.

(4) Soil pH, organic matter, available phosphorus, and urease activity are key factors linking environmental changes with microbial community succession. Medium-dose application (4.7 $kg \cdot m^{-2}$) demonstrated optimal balance between benefits and risk control and is thus recommended.

This study provides a practical framework for utilizing fungal cultivation wastes in plantation forests, contributing to circular bioeconomy and sustainable forest management goals. Future studies

 doi:10.20944/preprints202602.2049.v1

should extend monitoring periods to reveal long-term effects of SMS application and integrate plant growth responses to validate agronomic efficacy of recommended application rates.

Supplementary Materials: The following supporting information can be downloaded at the website of this paper posted on Preprints.org. **Figure S1.** Detailed map of the experimental site at Hushan Forest Station, Fuyang District, Hangzhou, Zhejiang Province. The red circle indicates the location of the nine experimental plots. **Table S2.** Full results of linear mixed models for all soil physicochemical properties and enzyme activities, including main effects and interactions (treatment, time, layer, and all two-way and three-way interactions). **Figures S2–S4.** Interaction plots for topsoil total phosphorus (TP), available phosphorus (AP), and urease activity (UA) across treatments and time points. **Table S3.** Differential abundance analysis (DESeq2) of bacterial and fungal phyla between treatments and time points. **Table S4.** Detailed nutrient composition of *Morchella sextelata* spent mushroom substrate used in this study, including comparative data with other common mushroom substrates.

Author Contributions: Conceptualization, B.W. and J.X.; methodology, B.W. and J.X.; software, B.W.; validation, B.W. and J.X.; formal analysis, B.W.; investigation, B.W.; resources, J.X. and J.Z.; data curation, B.W.; writing—original draft preparation, B.W.; writing—review and editing, J.X. and X.W.; visualization, B.W.; supervision, J.X.; project administration, J.X.; funding acquisition, J.X. All authors have read and agreed to the published version of the manuscript.

Funding: This work was supported by the National Key R&D Program of China (2023YFD220120303-01) for research on eco-efficient cultivation technologies in bamboo-based agroforestry systems (bamboo–tea, bamboo–mushroom, and bamboo–medicinal plant), and by the Science and Technology Project of the Zhejiang Provincial Forestry Department (2025B04) for promotion of semi-wild understory cultivation technology for morels in bamboo forests.

Institutional Review Board Statement: Not applicable.

Informed Consent Statement: Not applicable.

Data Availability Statement: The data presented in this study are available on request from the corresponding author.

Acknowledgments: The authors gratefully acknowledge the Miaoshanwu Experimental Forest Farm of the Research Institute of Subtropical Forestry for their assistance with field experiments. We also thank Guangzhou Gidiou Biotechnology Co., Ltd. for sequencing services.

Conflicts of Interest: The authors declare no conflicts of interest.

Abbreviations

The following abbreviations are used in this manuscript:

SMS	Spent mushroom substrate
TP	Total phosphorus
AP	Available phosphorus
AK	Available potassium
TN	Total nitrogen
SOM	Soil organic matter
EC	Electrical conductivity
UA	Urease activity
SA	Sucrase activity
ACP	Acid phosphatase
CAT	Catalase
APR	Acid protease
PCoA	Principal coordinate analysis
PERMANOVA	Permutational multivariate analysis of variance
LEfSe	Linear discriminant analysis effect size
ANOVA	Analysis of variance

 doi:10.20944/preprints202602.2049.v1

References

1. FAO. (2025). Global mushroom production statistics. Food and Agriculture Organization.
2. Sheer, A., Sardar, M. F., Younas, F., et al. (2024). Trends and social aspects in the management and conversion of agricultural residues into valuable resources: A comprehensive approach to counter environmental degradation, food security, and climate change. *Bioresource Technology*, *394*, 130258.
3. Tang, Q., Liu, W., Huang, H., et al. (2024). Responses of Crop Yield, Soil Fertility, and Heavy Metals to Spent Mushroom Residues Application. *Plants*, *13*(5), 663.
4. Zhao, F., Shi, S., Meng, R., et al. (2023). Soil Habitats Are Affected by Fungal Waste Recycling on Farmland in Agro-Pastoral Ecotone in Northern China. *Agronomy*, *13*(9), 2432.
5. Idowu, O. O., Akintola, O. A., Emmanuel, O. C., et al. (2023). Utilization of spent mushroom wastes as an alternative to use of inorganic fertilizer. *International Journal of Vegetable Science*, *29*(6), 516-526.
6. Zhang, B., Su, S., Chen, F., et al. (2015). Effects of mulch with mushroom residue on soil enzyme activities and soil physical-chemical property in Corylus orchard. *Nonwood Forest Research*.
7. Yuan, X., Qin, H., Wang, Y., et al. (2026). Coupled Effects of Tree Species and Understory Morel on Modulating Soil Microbial Communities and Nutrient Dynamics. *Microorganisms*, *14*(1), 99. PMID: 41194727
8. Sunil, C., & Xu, B. (2022). Mycochemical profile and health-promoting effects of morel mushroom Morchella esculenta (L.) – A review. *Food Research International*, *159*, 111571.
9. Wu, H., Chen, J., Li, J., et al. (2021). Recent Advances on Bioactive Ingredients of Morchella esculenta. *Applied Biochemistry and Biotechnology*, *193*(12), 4197-4213.
10. Li, J., Wu, H., Liu, Y., et al. (2021). The chemical structure and immunomodulatory activity of an exopolysaccharide produced by Morchella esculenta under submerged fermentation. *Food & Function*, *12*(19), 9327-9338.
11. Gao, C., Liu, P., Li, W., et al. (2025). Preparation of Morchella esculenta protein and its preventive effect on nonalcoholic fatty liver disease in mice. *Food & Function*, *16*(3), 1086-1099.
12. Wang, C. Y. (2020). A review on the potential reuse of functional polysaccharides extracted from the by-products of mushroom processing. *Food and Bioprocess Technology*, *13*(2), 217-228.
13. Törős, G., El-Ramady, H., Abdalla, N., et al. (2025). Valorization of Mushroom Residues for Functional Food Packaging. *International Journal of Molecular Sciences*, *26*(22), 10870.
14. Domínguez-Núñez, J. A., & Oliet, J. A. (2022). Management of mushroom resources in Spanish forests: a review. *Forestry: An International Journal of Forest Research*, *96*(2), 135-154.
15. Fierer, N. (2017). Embracing the unknown: disentangling the complexities of the soil microbiome. *Nature Reviews Microbiology*, *15*(10), 579-590.
16. Bose, T., Vivas, M., Slippers, B., et al. (2023). Retention of post-harvest residues enhances soil fungal biodiversity in Eucalyptus plantations. *Forest Ecology and Management*, *532*, 120806.
17. Kielak, A. M., Barreto, C. C., Kowalchuk, G. A., et al. (2016). The ecology of Acidobacteria: moving beyond genes and genomes. *Frontiers in Microbiology*, *7*, 744.
18. Tan, X., Cao, J., Liu, J., et al. (2024). Characteristics of three organic fertilizers and their influence on the mobility of cadmium and arsenic in a soil-rice (Oryza sativa L.) system. *Environmental Science and Pollution Research*, *31*(37), 49469-49480.
19. Mawarda, P. C., Le Roux, X., Dirk van Elsas, J., et al. (2020). Deliberate introduction of invisible invaders: A critical appraisal of the impact of microbial inoculants on soil microbial communities. *Soil Biology and Biochemistry*, *148*, 107874.
20. Wei, Z., Liu, L., Lei, Y., et al. (2024). Establishment of Pinus massoniana–Lactarius hatsudake Symbiosis. *Forests*, *15*(4), 578.
21. Leonardi, M., Furtado, A. N. M., Comandini, O., et al. (2020). Halimium as an ectomycorrhizal symbiont: new records and an appreciation of known fungal diversity. *Mycological Progress*, *19*(12), 1495-1509.
22. Phanpadith, P., Yu, Z., Yu, D., et al. (2019). Promotion of maize growth by a yellow morel, Morchella crassipes. *Symbiosis*, *80*(1), 33-41.
23. Kang, X., Liu, T., Li, J., Martin, F.M., Tan, H., et al. (2025). Biochar amendment improves Morchella sextelata yield by enhancing soil NO_3^--N availability and increasing fungal diversity. *Microbiological Research*, *302*, 128325. PMID: 40913927
24. Virk, A.L., Shakoor, A., Ahmad, N., Du, H., Chang, S.X., Cai, Y. (2025). Organic amendments restore soil biological properties under pesticides application. *Pesticide Biochemistry and Physiology*, *210*, 106394. PMID: 40262872

 doi:10.20944/preprints202602.2049.v1

25. Wu, Y., Qi, L., et al. (2026). Soil calcium ion enrichment associated with altered microbial functional gene networks in bamboo forest expansion. *Applied Soil Ecology*, *218*, 106685. DOI: 10.1016/j.apsoil.2025.106685
26. Li, S., et al. (2025). Comparative analysis of soil properties before and after Morchella sextelata cultivation across various soil types. *Frontiers in Microbiology*, *16*, 1700246. PMC12602436
27. Nuralykyzy, B., Nie, J., Mei, H., Zhang, Y., Rogers, K.M., Li, C., Yuan, Y. (2025). Synergies between Carbon Sequestration, Nitrogen Utilization, and Mushroom Quality: A Comprehensive Review. *Journal of Agricultural and Food Chemistry*, *73*(23), 14144-14157. PMID: 40406890
28. Quisth, I., Ulfsparre, I., Müller, B., Passoth, V., Solberg, S.Ø., Martín, C., Romero-Soto, L.A., Pent, M., Mousavi, H. (2026). Spent mushroom substrate (SMS) as a sustainable soil amendment and biofertilizer: A review. *Agricultural and Food Science*, *34*(4), 323-338. DOI: 10.23986/afsci.163895
29. Yang, Z.Y., Zhao, J.C., Ni, H.J. (2025). Silkworm excrement organic fertilizer substitution compound fertilizer improves bamboo shoot yield by altering soil properties and bacterial communities of Moso bamboo forests. *Frontiers in Plant Science*, *16*, 1550946. DOI: 10.3389/fpls.2025.1550946
30. Huang, Z., et al. (2025). On- and off-year management-induced changes in microbial communities cause microbial necromass carbon variation in subtropical Moso bamboo forests. *Applied Soil Ecology*, *204*, 105722. DOI: 10.1016/j.apsoil.2025.105722
31. Richardson, A. E., & Simpson, R. J. (2011). Soil microorganisms mediating phosphorus availability. *Plant Physiology*, *156*(3), 989-996.
32. Negassa, W., & Leinweber, P. (2009). How does the Hedley sequential phosphorus fractionation reflect impacts of land use and management on soil phosphorus: a review. *Journal of Plant Nutrition and Soil Science*, *172*(3), 305-325.
33. Blagodatskaya, E., & Kuzyakov, Y. (2008). Mechanisms of real and apparent priming effects and their dependence on soil microbial biomass and community structure: critical review. *Biology and Fertility of Soils*, *45*(2), 115-131.
34. Burns, R. G., DeForest, J. L., Marxsen, J., et al. (2013). Soil enzymes in a changing environment: Current knowledge and future directions. *Soil Biology and Biochemistry*, *58*, 216-234.
35. Sinsabaugh, R. L. (2010). Phenol oxidase, peroxidase and organic matter dynamics of soil. *Soil Biology and Biochemistry*, *42*(3), 391-404.
36. Nannipieri, P., Giagnoni, L., Landi, L., et al. (2011). Role of phosphatase enzymes in soil. In E. Bünemann, A. Oberson, & E. Frossard (Eds.), *Phosphorus in Action: Biological Processes in Soil Phosphorus Cycling* (pp. 215-243). Springer Berlin Heidelberg.
37. Hartmann, M., Frey, B., Mayer, J., et al. (2015). Distinct soil microbial diversity under long-term organic and conventional farming. *The ISME Journal*, *9*(5), 1177-1194.
38. Floudas, D., Binder, M., Riley, R., et al. (2012). The Paleozoic origin of enzymatic lignin decomposition reconstructed from 31 fungal genomes. *Science*, *336*(6089), 1715-1719.
39. Eilers, K. G., Debenport, S., Anderson, S., et al. (2012). Digging deeper to find unique microbial communities: the strong effect of depth on the structure of bacterial and archaeal communities in soil. *Soil Biology and Biochemistry*, *50*, 58-65.
40. Rousk, J., Bååth, E., Brookes, P. C., et al. (2010). Soil bacterial and fungal communities across a pH gradient in an arable soil. *The ISME Journal*, *4*(10), 1340-1351.
41. Hao, H., Yue, Y., Chen, Q., et al. (2024). Effects of an efficient straw decomposition system mediated by Stropharia rugosoannulata on soil properties and microbial communities in forestland. *Science of The Total Environment*, *916*, 170226.
42. Liu, Q., He, G., Wei, J., et al. (2021). Comparative transcriptome analysis of cells from different areas reveals ROS responsive mechanism at sclerotial initiation stage in Morchella importuna. *Scientific Reports*, *11*(1).
43. Miina, J., Muttilainen, H., Vornanen, J., et al. (2023). Supply Chain Actors' Perspectives Concerning the Cultivation of Specialty Wood-Decay Mushrooms in Finland. *Forests*, *14*(1), 134.
44. Legendre, P., & Legendre, L. (2012). *Numerical Ecology* (3rd ed.). Elsevier.